MODELING, IDENTIFICATION AND CONTROL, 1981, VOL. 2, NO. 1, 37–56

An implementation of estimation techniques to a hydrological model for prediction of runoff to a hydroelectric power station

MAGNE FJELD† and SVERRE AAM‡

Keywords: *state estimation, parameter estimation, Nordic hydrological model, run-off prediction, hydroelectric power production.*

Parameter and state estimation algorithms have been applied to a hydrological model of a catchment area in southern Norway to yield improved control of the household of water resources and better economy and efficiency in the running of the power station, as experience proves since the system was installed on-line in the summer of 1978.

A non-linear conceptual state-space model of a Nordic hydrological system is presented in this paper. The model is transformed analytically to a piecewise linear time-discrete form in order to obtain straightforward updating of the gain matrix in the estimator through solution of the Riccati equation. Estimator gains can then be expressed approximately as a function of the state. Discharge coefficients (time constants) are estimated by the maximum likelihood method. Results are presented which show estimated and observed run-offs, and estimates of the state variables.

1. Introduction

Electric power production in Norway is entirely hydroelectric. Lately, there has been public pressure to reduce the need for further utilization of the remaining water resources. This fact has motivated an increased interest for improved economy in and better utilization of the existing hydroelectric power production systems. Some 8–9 years ago, the authors suggested that the benefits derived by taking into account the hydrological dynamics which are environmental to the power station basins could be significant (Fjeld and Sande 1972, Fjeld, Meyer and Aam 1973). Introductory studies at University level were done, which demonstrated that the hydrological dynamics of the environment, i.e. the complete catchment area, could be very significant indeed for short and medium planning terms for optimal dispatch of the available water energy. A pilot study on the mathematical modelling of a Nordic hydrological system was done, along with a computational example on how a simplified run-off model could be used in the optimal control of the most economical dispatch of the power (Fjeld, Meyer and Aam 1973). Eventually, this contributed to an increased national interest in the hydrological modelling aspects in the framework of either the state-space approach using conceptual models, coupled with the stochastic

---

Received 14 May 1980. This paper has been published in *I.E.E.E. Trans. autom. Control*, **25**, April 1980 and is reprinted in *MIC* with the permission of the authors and the publisher.

† Affiliation at project time: SINTEF, Division of Automatic Control, N-7034 Trondheim-NTH, Norway. From 1 February, 1979: AccuRay Corporation, P.O. Box 02248, Columbus, Ohio 43202, U.S.A.

‡ Present address: Norwegian Research Institute of Electricity Supply (EFI), N-7034 Trondheim-NTH, Norway.

nature of the inputs, or input/output models which merely tried to reproduce the observed outputs caused by observed inputs in a stochastic environment.

The use of AR and ARMA models in prediction of river flows, run-off and so forth has been reported for some years (see, for example, Kashyap and Rao 1972, Vansteenkiste 1976). Of conceptual models, i.e. models developed on mass balance and physical arguments and descriptions related to the process, the Stanford watershed models are probably the most well known (Crawford and Linsley). Models of the Stanford type give a rather detailed and satisfactory explanation of hydrological phenomena, but due to the large number of unidentifiable parameters such models introduce, they are not suitable, or overparametrized for estimation and prediction purposes for an actual hydrologic basin.

Linear ARMA models are partly inadequate under Nordic conditions, if the model is to cover all seasons. The inclusion of freezing and snow melting during the winter season implies either a change of structure or large parametric changes in a model (depending on the viewpoint). The early work done (Meyer 1972) and later published (Fjeld, Meyer and Aam 1973) suggested a simpler structure which is reasonably well observable with respect to unknown parameters, and which took account of freezing and melting. A still simpler model, and it seems a model sufficiently adequate for our purposes, was presented by Bergerström and co-workers (Bergström and Forsman 1973, Bergström 1975), in the form of schematic block diagrams and FORTRAN routines, the so-called HBV-model.

In 1976, two Norwegian hydroelectric power companies together with the State Power Company (NVE/Statskraftverkene) agreed to finance a project on application and implementation of a hydrological model, to yield run-off predictions to the short term reservoirs of a power station.

The catchment basin of the Tonstad power station at the Sira-Kvina river in southern Norway was chosen for this project. This power station produces, on an average, electric power worth $75 million per year. The important characteristics of the power station reservoir in this system is that it has a small degree of autonomous regulation, i.e. small volumes compared to inflow, and further that the pressure head at the turbine intakes is large and significantly dependent on the reservoir level. Hence, there is a trade-off between keeping as much water as possible in the reservoirs in order to gain production efficiency, and risk of spilling water due to flooding. This problem is dealt with by appropriate optimization and interactive simulation programs. However, such programs require reliable prediction of the run-off from 1 to 5 days ahead. At the Tonstad power station, the predictions for the natural, unregulated run-off are used in a complete simulation model of the total hydropower system, encompassing the unregulated and regulated flows, in order to reach short-term rational decisions on how to run the power stations.

Among hydrologists, the problem of how to update dynamical run-off models against field measurements has been recognized as a difficult problem, and some have designed intuitive methods to combat the problem. However, the Kalman state estimator approach proves to be an elegant and simple recursive method for accomplishing the required updating, in order to obtain a best possible prediction of the state variables and run-off for the next few days. 'The best possible' certainly does not imply 'optimal' in conjunction with the Nordic hydrological model of a complex system like the one we deal with here. It does mean, however, that the recursive method applied is a simple and practical one, and based on a more theoretically sound basis than intuitive approaches.

2. State space model description

The HBV-3 model (Bergström and Forsman 1973, Bergström 1975) is relatively simple, in that it describes coarsely the behaviour of the snow magazine, the soil moisture zone, an intermediate zone and the groundwater zone. The model is composed of these in cascade with each other. The lower zones are divided in two parts, an upper zone and a groundwater zone. The latter is lumped together with possible lake volumes (see the schematic diagram of Fig. 1). In the original publications of Bergström and Forsman (1973) and Bergström (1975) the basic model description was developed and given as diagrams and FORTRAN subroutines. For estimation and prediction purposes, it is necessary to translate such a description into the state variable form, which is not common in hydrology. We will, in the following, look at each particular section of the model, but we are not going to discuss here the relevance of the model structure and the various non-linearities aiming at simulating nature's behaviour.

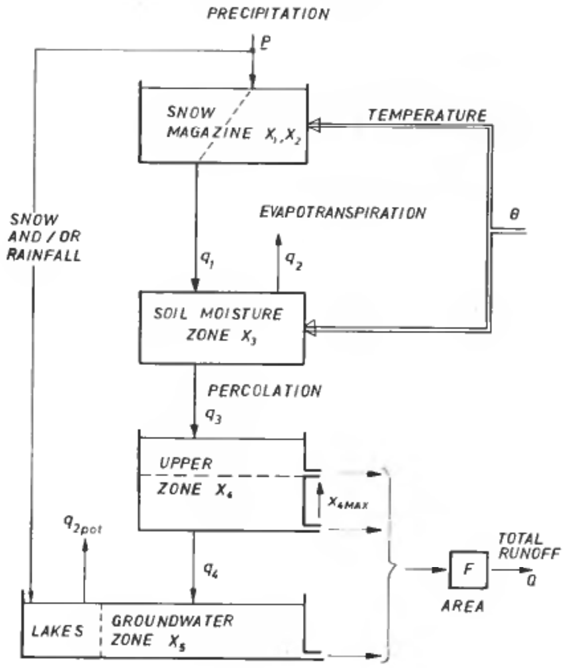

Figure 1. Per unit area model of a Nordic Hydrological System (HBV-model).

2.1. *The snow magazine*

This magazine is characterized by two state variables, namely, the water equivalent x_1 of dry (frozen) accumulated snow, and the content x_2 of free water stored in the snow. See Fig. 2.

If the temperature is less than θ_W, the precipitation $P(t)$ will fall as snow, otherwise it will be rain. Although the rate of melting snow of is dependent on many factors, it is here considered to be controlled directly by the ambient temperature and without any inherent dynamics beyond the rate controlling behaviour. Therefore, it is assumed that the melting rate is equal to $C_0(\theta(t)-\theta_0)$, where $\theta(t)$ is taken to be the

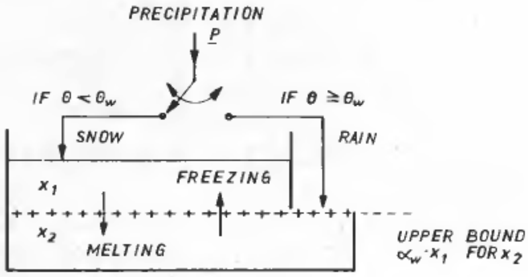

Figure 2. Snow magazine model.

mean daily temperature. The water accrued from melting can increase the water content x_2 up to a certain level, then the snow is saturated with water. Only when such a condition is satisfied, the water can run-off to the soil moisture zone. We simplify the description in this paper by putting $\theta_0 = \theta_W$, and obtain

$$\dot{x}_1(t) = \begin{cases} P(t) - C_0(\theta(t) - \theta_0) & \text{for } (a)\text{: } \theta \leqslant \theta_0, \quad x_1 \geqslant 0, \quad x_2 > 0 \\ -C_0(\theta(t) - \theta_0) & \text{for } (b)\text{: } \theta > \theta_0, \quad x_1 > 0, \quad x_2 > 0 \\ P(t) & \text{for } (c)\text{: } \theta \leqslant \theta_0, \quad x_1 \geqslant 0, \quad x_2 = 0 \\ 0 & \text{for } (d)\text{: } \theta > \theta_0, \quad x_1 = 0 \end{cases} \tag{1}$$

$$x_2(t) = \begin{cases} C_0(\theta(t) - \theta_0) & \text{for } (e)\text{: } \theta \leqslant \theta_0, \quad x_2 > 0 \\ P(t) + C_0(\theta(t) - \theta_0) & \text{for } (f)\text{: } \theta > \theta_0, \quad x_2 < \alpha_W x_1 \\ 0 & \text{for } (g)\text{: } \theta \leqslant \theta_0, \quad x_2 = 0 \\ -\alpha_W C_0(\theta(t) - \theta_0) & \text{for } (h)\text{: } \theta > \theta_0, \quad x_2 = \alpha_W x_1 > 0 \end{cases} \tag{2}$$

The flow rate q_1 to the soil moisture zone will be

$$q_1(t) = \begin{cases} 0 & \text{for } x_2 < \alpha_W x_1, \quad x_1 > 0, \quad x_2 > 0 \\ (1 + \alpha_W) C_0(\theta(t) - \theta_0) + P(t) & \text{for } \theta > \theta_0, \quad x_2 = \alpha_W x_1 > 0 \\ P(t) & \text{for } \theta > \theta_0, \quad x_1 = x_2 = 0 \end{cases} \tag{3}$$

In the catchment area we consider here, there are large altitude variations. It is a characteristic that, on average, the temperature decreases with altitude, and the precipitation increases. Descriptions of these phenomena are available, and we include this knowledge in the model by making a *distributed model* of the snow accumulation and melting, by dividing the catchment area according to contiguous altitude segments $[h_1 - \Delta h_1, h_1 + \Delta h_1]$, . . ., $[h_N - \Delta h_N, h_N + \Delta h_N]$. The corresponding temperature at altitude h_i is denoted by θ_i.

It is easily demonstrated that none of the states x_1 and x_2 are locally observable through a measurement of q_1 (if measurement of q_1 was possible), and even less so in the distributed model.

Hence, no measurement of run-off in the hydrological model we are considering can locally recover the magnitudes of stored dry snow and water. However, this does not mean that these states are impossible to estimate in an open-loop manner if we know initial conditions, and are able to measure the inputs θ and P. After the summer season, we simply know that $x_1 = x_2 = 0$. Hence, the functions $x_1(\cdot)$ and $x_2(\cdot)$ can be computed without updating. The multi-altitude snow magagine model is included in the estimator described later, but for readability, we do not make reference to it any more in the paper.

2.2. *The soil moisture zone*

This zone represents the upper porous soil layer. Some water will disappear from this layer due to evapo-transpiration (evaporation and transpiration of water from vegetation).

If the water content x_3 in the soil moisture zone is equal to its saturation value $x_{3\max}$, the water flows on to the upper zone. If, however, the water content is less than $x_{3\max}$, the run-off to the upper zone is given by the product $(x_3/x_{3\max})^{\beta} q_1$, the balance being stored in the zone.

The evapo-transpiration is computed from a potential (maximal) value $q_{2\text{pot}}$, which is dependent on many factors. The actual value is assumed linearly dependent on x_3 up to $q_{2\text{pot}}$ at $x_3 = x'_{3\max}$. As a simplification, we put $x'_{3\max} = x_{3\max}$ from now on.

Summing up, the state differential equation for the soil moisture zone is

$$\dot{x}_3(t) = q_1(t) - m(x_3) q_1(t) - (1 - \alpha(t)) q_2(x_3(t), t) \tag{4}$$

where

$$m(x_3) = \begin{cases} \left(\dfrac{x_3}{x_{3\max}}\right)^{\beta} & \text{for} \quad 0 < x_3 < x_{3\max} \\ 1 & \text{for} \quad x_3 \geqslant x_{3\max} \end{cases}$$

$$q_2(x_3(t), t) = \begin{cases} q_{2\text{pot}}(t) & \text{for} \quad x_3 \geqslant x_{3\max} \\ \left(\dfrac{x_3}{x_{3\max}}\right) q_{2\text{pot}}(t) & \text{for} \quad x_3 < x_{3\max} \end{cases} \tag{5}$$

$\alpha(t)$ = average fraction of surface covered by snow.

$q_{2\text{pot}}(t)$ is given by hydrological estimates or measurements, and its magnitude for a given field can be assumed to be approximately governed by the temperature. However, in a Nordic climate, the evapo-transpiration is not as important as it would be in a tropical area.

2.3. *The upper and groundwater zones*

The two compartments representing these zones constitute almost the simplest way to model the dominant non-linear behaviour of the run-off from a catchment area. They also constitute a coarse representation of the infiltration of water through the various layers of soil. As an approximation, lakes are assumed to be in direct non-dynamic connection with the lower zone. Also, during the winter season, the loading effect of snow and ice, causing a transfer of lake water to the groundwater zone, is being modelled.

The equations for the upper and lower groundwater zones are

$$\dot{x}_4(t)=\begin{cases} -a_1(x_4(t)-x_{4\max})-a_2x_4(t)+q_3(t)-\dfrac{q_4}{1-\alpha_L} & \text{for} \quad x_4>x_{4\max} \\ -a_2x_4(t)+q_3(t)-\dfrac{q_4}{1-\alpha_L} & \text{for} \quad x_4\leqslant x_{4\max} \end{cases} \tag{6}$$

$x_{4\max}$ is a threshold value of x_4, for which the discharge time constant is $1/(a_1+a_2)$, whereas it is $1/a_2$ for $x_4 \leqslant x_{4\max}$.

As a simplification, q_4 is taken as a constant flow rate, as long as $x_4(t)>0$. For the lower zone

$$\dot{x}_5(t)=-a_3x_5(t)+q_4+\alpha_L(p(t)-q_{2\text{pot}}) \tag{7}$$

$1/a_1$ and $1/a_2$ are the time constants associated with the upper zone, whereas $1/a_3$ is the time constant associated with the lower zone. α_L is the fractional area covered by lakes.

2.4. *The run-off from the catchment area*

The total run-off from the basin follows from Fig. 1.

$$Q(t)=\begin{cases} [a_1(x_4(t)-x_{4\max})+a_2x_4](1-\alpha_L)F+Fa_3x_5(t) & \text{for} \quad x_4>x_{4\max} \\ a_2x_4(t)(1-\alpha_L)F+Fa_3x_5(t) & \text{for} \quad x_4\leqslant x_{4\max} \end{cases} \tag{8}$$

where F is the total area of the catchment.

Units of all state variables are in volume per unit area, in hydrology usually given in units of 10^{-3} m. Rates and flow rates are hence given as 10^{-3} m/unit time, in hydrology usually as 10^{-3} m/day.

3. The modelling of the measurements

3.1. *Run-off*

This variable is in the field measured as accumulated run-off over 24 hours, i.e. the measurement is a time-discrete value given by

$$y(k\Delta T)=\int_{(k-1)\Delta T}^{k\Delta T} Q(t)\,dt; \quad k=1,2,3,\ldots \tag{9}$$

whereas the model output is a run-off intensity $Q(t)$. An approximate discrete-time model version of the measurement process is therefore

$$y(k)\cong[Q(k)+Q(k-1)]\frac{\Delta T}{2} \tag{10}$$

where we have for convenience used k as argument instead of $k\Delta T$.

3.2. *Precipitation*

This input variable is, of course, never measured in the field as an intensity either, but as an accumulated value $r(k)$ over 24 hours, such that

$$P(k)\cong\frac{2}{\Delta T}r(k)-P(k-1) \tag{11}$$

$P(k)$ is usually given in units of 1 m^{-3}/unit area and 24 hours.

Temperature data are given as average daily values, and *evapo-transpiration* data are given on a monthly basis.

4. Discrete-time system equation

In order to formulate the discrete-time Kalman estimator for the locally linearized system, it is convenient to find analytically a locally valid expression for the process state transition matrix Φ, since Φ is needed in the computation of the $n \times 1$ estimator gain matrix K. Owing to the special structure of the process model, this is quite straightforward. The result is derived in the Appendix, and has the form

$$x(k+1)=\Phi(B(x(k), \theta(k)), P(k), \theta(k), q_{2\text{pot}}(k), \Delta T)x(k) + \tilde{u}(B(x(k), \theta(k)), P(k), \theta(k), q_{2\text{pot}}(k), \Delta T) \qquad (12)$$

where the function B is defined in the Appendix.

The entries of Φ and the components of $\tilde{u}$ are given in the Appendix. Similarly, the ideal observation process is given by a piecewise constant observation matrix D and the following expression:

$$y(k)=Dx(k)+y_0 \qquad (13)$$

where

$$D=\begin{cases}\left[0, 0, 0, F(1-\alpha_L)(a_1+a_2)\dfrac{\Delta T}{2}, Fa_3\dfrac{\Delta T}{2}, \dfrac{\Delta T}{2}\right] & \text{for} \quad x_4 \geqslant x_{4\max} \\ \left[0, 0, 0, F(1-\alpha_L)a_2\dfrac{\Delta T}{2}, Fa_3\dfrac{\Delta T}{2}, \dfrac{\Delta T}{2}\right] & \text{for} \quad x_4 \leqslant x_{4\max}\end{cases} \qquad (14)$$

y_0 is a piecewise constant such that

$$y_0=\begin{cases}-a_1 x_{4\max}(1-\alpha_L)F\dfrac{\Delta T}{2} & \text{for} \quad x_4 > x_{4\max} \\ 0 & \text{for} \quad x_4 \leqslant x_{4\max}\end{cases} \qquad (15)$$

Again the formulations (13), (14) and (15) make a computation of the locally valid values of the covariance and gain matrices of the Kalman estimator possible.

5. Local state observability: structure of the estimator

From the structure of the process state equations, it is easy to prove, using the well-known observability matrix condition, that x_1 and x_2 are not locally observable from the output measurement y. With the assumed model, the run-off from the snow magazine is independent on inputs only and not on the magnitudes of the state variables as long as x_1 and $x_2 > 0$. Hence, even with data on melting, it is impossible to infer conclusion locally on the magnitudes of x_1 and x_2. This statement cannot, of course, be globally true in general for the non-linear process where $x_1 \geqslant 0$, $x_2 \geqslant 0$. Indeed, if we can add to the model the information that all of the snow disappears every summer, one can certainly state that the accumulated total water content of the snow magazine finally must match the accumulated run-off and water contents x_3, x_4 and x_5, as seen between two summer seasons.

For short-term prediction, the practical scheme must be based on the best 'ballistic' estimate (i.e. without updating) of x_1 and x_2 based on temperature and precipitation measurements and the model eqns. (1) and (2). As a consequence, for the Kalman estimator design the complete hydrological model must be divided in a locally observable part (the soil and groundwater zones) and a locally non-observable part (the snow magazine). The structure of the system with estimator updating is as shown in Fig. 3. We applied the form of the Kalman filter that minimizes the expectation of the one-step-ahead predicted error criterion.

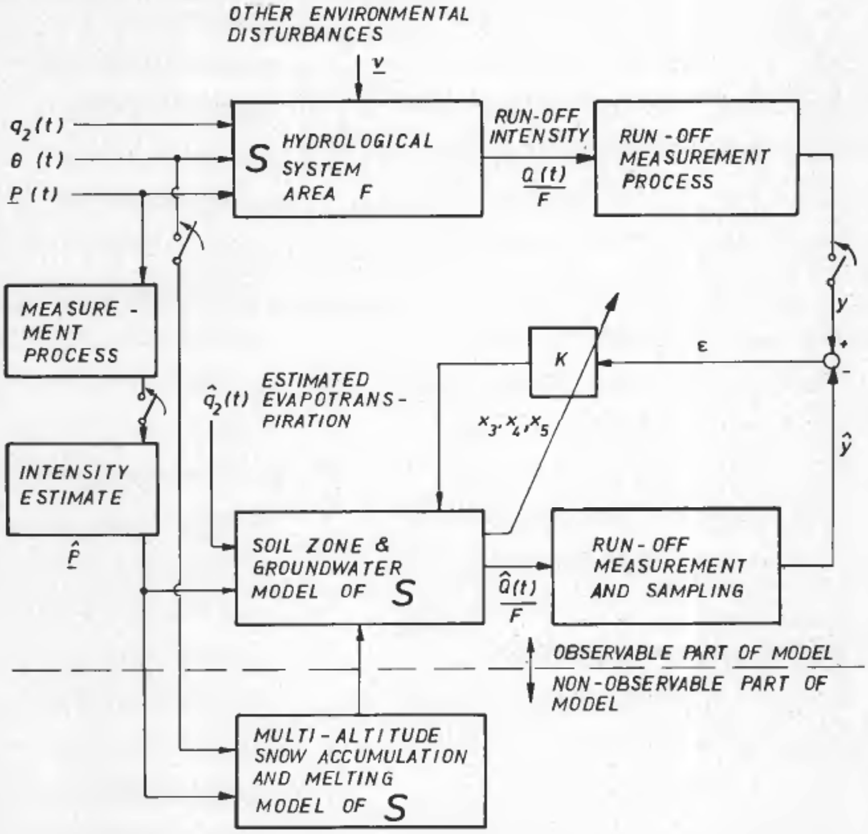

Figure 3. Structure of the estimation and updating scheme.

Practical experience has shown that an updating based on no information on the snow magazine whatsoever is unnecessarily restrictive, as explained above (see also § 8). The continuous non-linear model equations in the on-line Kalman estimator were solved by an accurate method between two sampling instants $k\Delta T$ and $(k+1)\Delta T$ in order to satisfy exactly conservation of the mass flow. With the computational power of a minicomputer, there is no need in this system to work with simplified schemes. Such a point is sometimes bypassed and unnoticed in texts and papers on implementations of filtering techniques.

6. Model calibration: simulations with the estimator

6.1. *Parameter identification*

Although the approximate range of parameter values of many of the HBV model parameters is transferable from other catchment areas that have been researched, it is certainly necessary to tune the parameters for the Sira-Kvina catchment model.

The parameters can be divided in three categories: those which can be found by studying the catchment area (total area, altitudes of partial areas for the snow magazine model, lakes, α), those physical parameters for which good *a priori* estimates exist (average variations in temperature and precipitation as a function of altitude, C_0, α_W, θ_0, θ_W), and finally, such parameters which values are almost not known at all although useful estimate ranges exist from studies of other catchment areas. Such parameters are x_{3max}, β, x_{4max}, q_4, a_1, a_2 and a_3.

For linear systems with zero mean gaussian additive process and measurement noise it is well known that the maximum likelihood (ML) estimate of the system parameters $\boldsymbol{p}$ is obtained by applying for the model with known inputs and an observed output time series Y_N over the time interval [1, N], (Schweppe 1973, Eykhoff 1974):

(1) a Kalman filter to yield the innovation sequence $\{\epsilon_k\}$ and its covariance R_k, for a fixed $\boldsymbol{p}$, over the time interval [1, N];

(2) a stepwise procedure whereby $\boldsymbol{p}$ is changed towards a value $\boldsymbol{p}_0$ that maximizes the likelihood functional $J = \ln p(Y_N/\boldsymbol{p})$;

(3) run step (1) again with the improved value for $\boldsymbol{p}$.

For non-linear models like the one we have, which is in fact piecewise linear except for the less important non-linear soil moisture zone, the method of course gives an approximation to the solution of the problem. The computations (1)–(3) were done using the program package MLPROG (Hallingstad 1976) contained in the interactive program system PROSID for time series analysis state and parameter estimation, which is a part of a cybernetic program library CYPROS (Tyssø 1977).

Considering equidistant plots of the error criterion in dependence of any two of the aforementioned parameters, applying either the maximum likelihood functional or the least-squares functional of the open-loop output prediction error, demonstrated that sensitivities in the criterion to changes in many parameters were low. This means that the degree of identifiability of those same parameters is low. For this reason, we considered it sufficient to calibrate the model in a two-step procedure.

(1) Apply a least-squares estimation of all of the ten unknown and approximately known parameters. This gave a course calibration of the model, although theoretically with biased estimates of parameters. Considering a weak identifiability (overparameterized model), this is considered good enough as final values for all parameters except a_1, a_2 and a_3 (the run-off discharge constants).

(2) Apply the ML method to yield final values for the run-off parameters a_1, a_2 and a_3.

We then arrived at the following parameter values:

$$C_0 = 5{\cdot}2\ [\mathrm{m}^{-3}\ (°\mathrm{C})^{-1}\ (\mathrm{day})^{-1}, \quad \alpha_w = 0{\cdot}08, \quad \theta_0 = 0{\cdot}0\ [°\mathrm{C}]$$

$$\theta_w = 0{\cdot}8\ [°\mathrm{C}], \quad x_{3max} = 50\ [\mathrm{m}^{-3}], \quad \beta = 2$$

$$q_4 = 2{\cdot}0\ [\mathrm{m}^{-3}\ (\mathrm{day})^{-1}]$$

$$x_{4max} = 20\ [\mathrm{m}^{-3}], \quad a_1 = 0{\cdot}547\ [\mathrm{day}^{-1}]$$

$$a_2 = 0{\cdot}489\ [\mathrm{day}^{-1}], \quad a_3 = 0{\cdot}0462\ [\mathrm{day}^{-1}]$$

In order to calculate the Kalman estimator gain, which was updated against the current values of Φ and D, we considered the model in the form (see Appendix)

$$\left.\begin{aligned} x(k+1) &= \Phi_{x,u}(k)x(k)+\bar{u}_{x,u}(k)+\tilde{u}(k) \\ y(k) &= D_x x(k)+y_{0x}+w(k) \end{aligned}\right\} \tag{16}$$

where $\{\tilde{u}(k)\}$ and $\{w(k)\}$ are assumed to be gaussian, white noise sequences with zero mean. Indices x and u are used to remind about the dependence on the working point. Updating of K is done through solution of the Riccatti equation one step at a time.

6.2. *Identifiability of parameters*

Following Tse (1974), an identifiability analysis of a_1, a_2 and a_3 was done. The eigenvalues and eigenvectors of Fisher's information matrix M_{p_0} give us some idea about the degree of identifiability of the unknown parameters $\boldsymbol{p}$. If the likelihood functional J is sufficiently smooth as a function of $\boldsymbol{p}$, then cov $\{\hat{p}_E\} \approx M_{p_0}{}^{-1}$ (lower bound), where p_E is an efficient estimate (Schweppe 1973), and

$$M_{p_0} = \underset{Y_N}{E}\left\{\frac{\partial J}{\partial p}\frac{\partial J}{\partial p^T}\right\}_{p=p_0}$$

where the bracket expression is the Hessian matrix H_{p_0}. In the MLPROG, H_{p_0} is found approximately through computation of the sensitivities

$$\frac{\delta J}{\delta p_i} = \frac{J(p+\Delta p_i)-J(p)}{\Delta p_i}$$

at the optimum $\boldsymbol{p}$ found by MLPROG.

From matrix theory, we know that $1/\sqrt{\lambda_i}$ is the length of a principal half axis of the ellipsoid $\frac{1}{2}p^T Hp=$constant, where λ_i is an eigenvalue of H. The associated eigenvectors $\boldsymbol{m}_i$ give us the direction of the principal axes. If now λ_i is small, the parameter combination corresponding to the direction of the eigenvector of λ_i is poorly identifiable. By calling the subroutine CURVE in MLPROG, the directions and length of the principal axes are computed. The result for the hydrological model is given in the Table.

Principal half axis	Eigenvalue	Direction		
1st	480	−0·967	0·254	0
2nd	828	−0·280	−0·960	0
3rd	40780	0	0	1

By computing the length of principal axes relative to parameter estimates, it is observed that a_3 is only slightly less observable than a_1 and a_2. The results indicate about equal observability of these parameters, since the principal axes, being proportional to $1/(\sqrt{\lambda_i}\hat{a}_i)$, are about orthogonal and the ellipsoid almost a sphere.

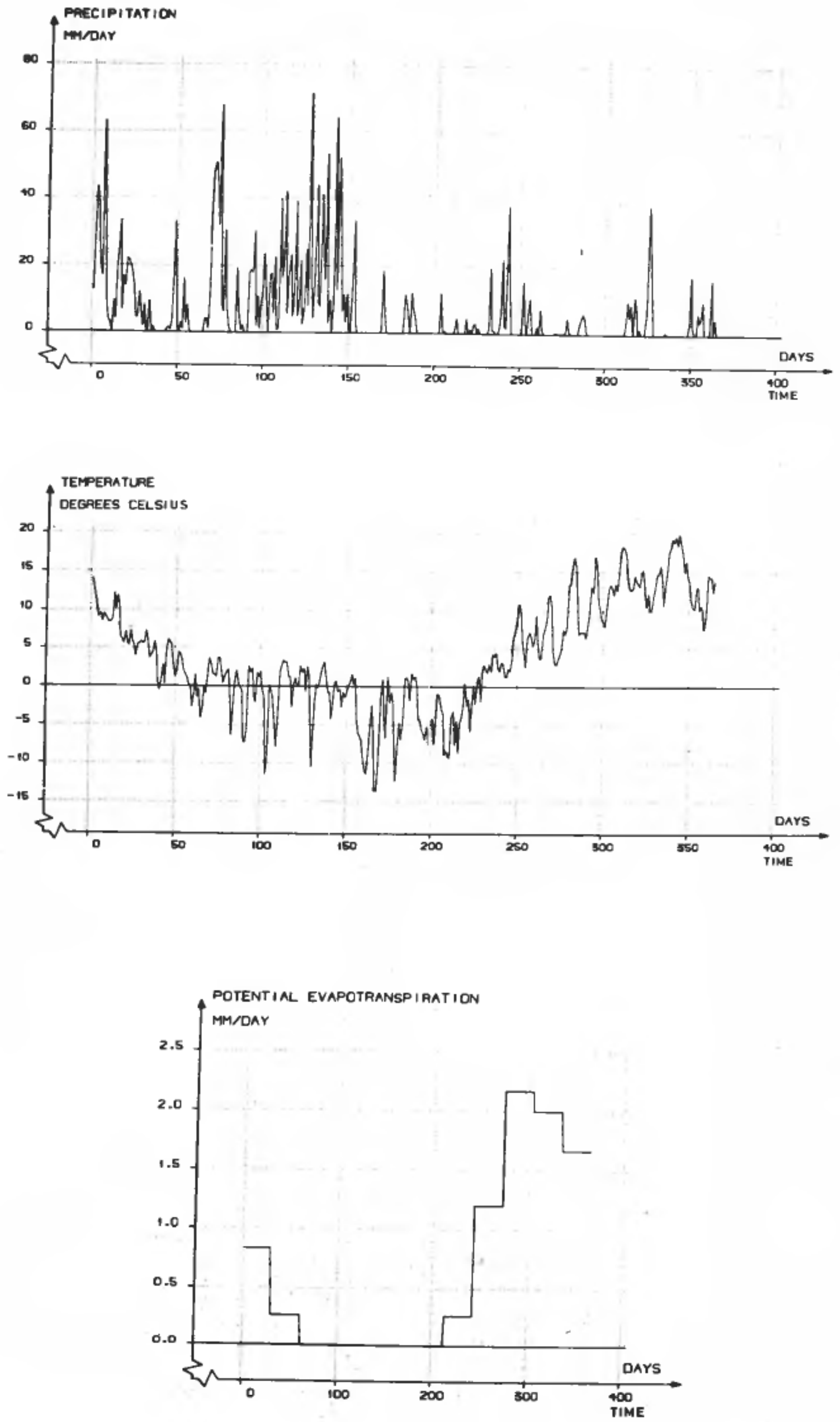

Figure 4. (*a*) Precipitation, (*b*) temperature, and (*c*) potential evapo-transpiration.

According to the above, lower bound (Cramer–Rao) estimates of the parameter uncertainties are given by

$$\hat{\sigma}_{a_1} \geqslant 100/(\sqrt{\lambda_1}\hat{a}_1)\% = 8{\cdot}3\%$$
$$\hat{\sigma}_{a_2} \geqslant 100/(\sqrt{\lambda_2}\hat{a}_2)\% = 7{\cdot}1\%$$
$$\hat{\sigma}_{a_3} \geqslant 100/(\sqrt{\lambda_3}\hat{a}_3)\% = 10{\cdot}7\% \ .$$

6.3. *Simplifications, simulations and comparisons*

In a practical implementation on a small multiprogrammed computer, there is a need for avoiding the necessity for solving the Riccati equation in order to update the filter $n \times 1$ gain matrix K. By inspection of the behaviour of each of the elements k_i of K, applying for its design cov $\{v\}$=diag $\{1, 1.1, 10, 0\}$ and cov $\{w\}=1$ in the observable part of the model, we have observed that the following good approximation can be made:

$$K \approx [0, k_{uz}(x_4), k_{gz}(x_4), 0]$$

for the gain elements associated with the states x_3 to x_6 respectively. We found

$$k_{uz} = \begin{cases} k_1 & \text{for} \quad x_4 > x_{4\max} \\ k_2 & \text{for} \quad x_4 \leqslant x_{4\max} \end{cases}$$

$$k_{gz} = \begin{cases} 0 & \text{for} \quad x_4 > 0 \\ k_3 & \text{for} \quad x_4 = 0 \end{cases}$$

A least-squares optimization of k_1, k_2 and k_3 to fit the Kalman filter run-off behaviour resulted in $k_1 = 0{\cdot}5$, $k_2 = 1{\cdot}6$ and $k_3 = 3{\cdot}4$.

These constants are used in the following, and we shall for simplicity refer to the filter as a 'Kalman filter', although it is a simplified one.

With the resulting model, and the observed temperature, measured precipitation and evapo-transpiration data as given in Figs. 4 (*a*)–(*c*), the following experiments were done. Figure 5 shows the observed run-off and the ballistic (i.e. without updating) run-off from the model for a period of one year, starting on 1 September 1974.

In Fig. 6, the same type of curves are shown, except that the model run-off there is generated by the Kalman filter. The error has been somewhat reduced, although the open-loop model is astonishingly good as judged from Fig. 5. Figure 7 (*a*) shows the innovation sequence. Some of the rapid, white-noise-like fluctuations are highly probable caused by random errors in the run-off observations. In fact, the total run-off from the catchment is calculated on the basis of the differences of measurements at different locations (in rivers), and this will give avoidable errors, in particular when the total flow on transit between two such locations is high compared to the net run-off.

A characteristic of such measurements is also that the measurement uncertainty increases somewhat with the magnitude of the measurement variable. In this implementation, this fact is, however, not taken into account in the estimator.

Another source of error is that melting of snow will be dependent not only on ambient temperature, but also the intensity of sun radiation hitting the snow, and wind has a significant effect too.

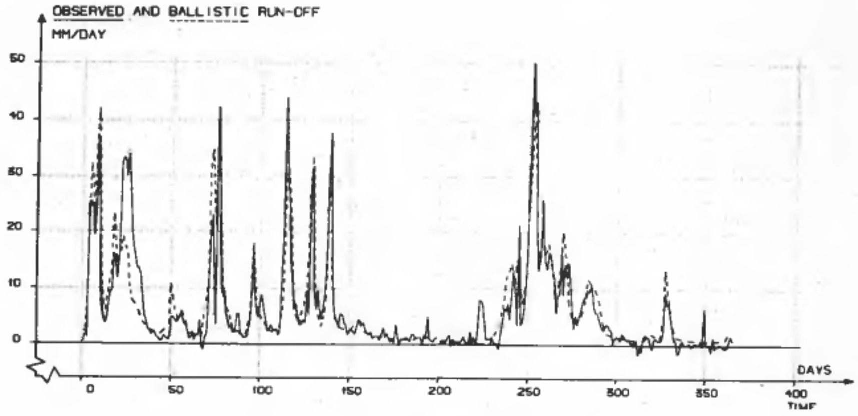

Figure 5. Observed and ballistic model run-off.

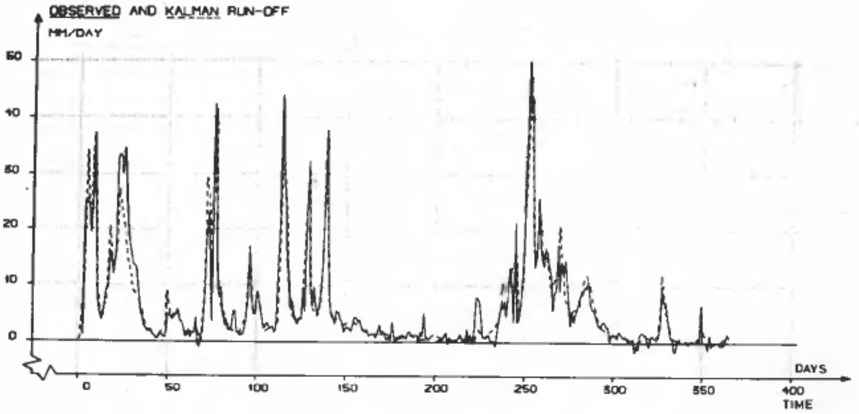

Figure 6. Observed Kalman filter run-off.

It should also be remarked that the measurement sampling interval is much too long. The updating frequency in this application causes poor updating of the fast modes, and this is one of the valuable results of the modelling and estimation work done. As a result, the power company will aim at increasing the updating frequency.

Figure 7 (*b*) shows the square of the innovation integrated as a function of time, with and without filter updating.

However, as an overall judgement, it is remarkable how well the run-off from a highly *distributed parameter* process like this can be satisfactorily modelled for the purpose here, by a relatively simple *lumped parameter* model. Discussing this in brief, it is tempting to relate this fact to the following. A hydrological basin with a major outgoing river could be divided in a number of smaller compartments that in many cases could be chosen such that there would be a minimum of interaction between them, and a maximum of direct flow to the observed run-off.

Rivers, streams and lakes could be natural borders of such compartments, which could with good accuracy (compared to the total catchment) be given a lumped mathematical description. As seen from the output, the main river from the catchment, the system then mainly encompasses parallel compartments each of which

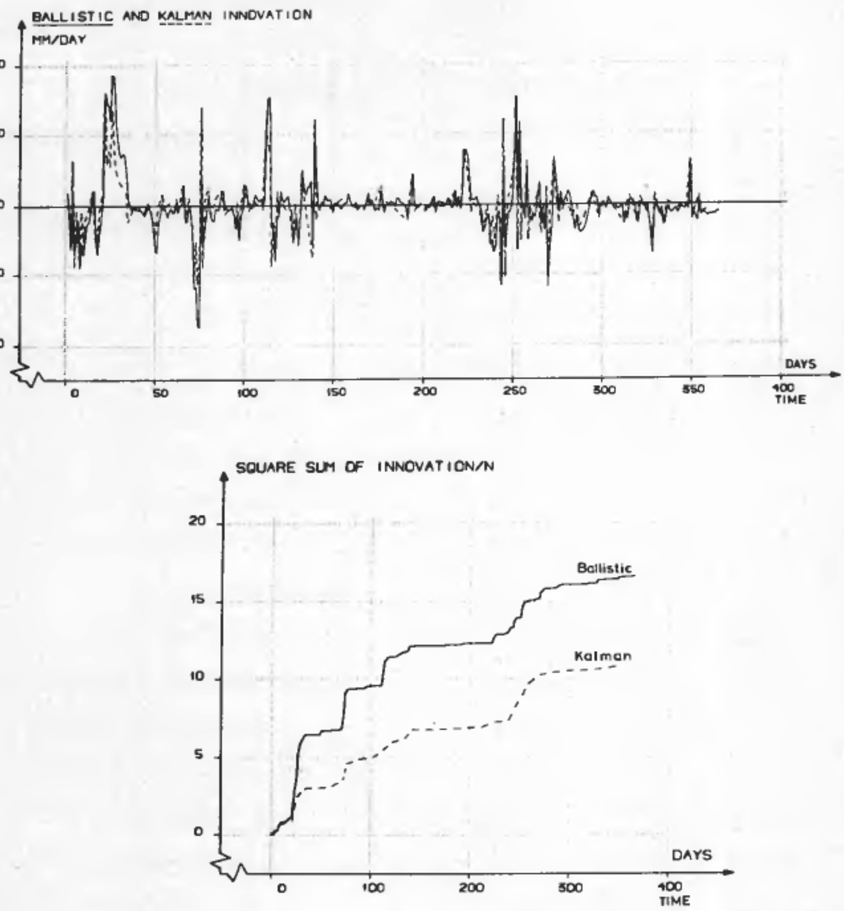

Figure 7. (*a*) The innovations, with ballistic model and with Kalman filter, (*b*) integral of the squared innovations, with ballistic model and with Kalman filter.

has a dynamic behaviour depending on hydrological parameters for that compartment. However, the dynamics of each will not differ very much, and in fact very little if the catchment is homogeneous. As a result, the response of the output will be the sum of almost equal and parallel responses governed by systems which will be practically state unobservable from the output. Hence, a simplified lumped description will suffice.

In Figs. 8 (*a*)–(*d*), the estimated values of x_1+x_2, and the states x_3 to x_5 are plotted, for the same input data as previously.

As an example, the behaviour of both the ballistic (open-loop) estimated value and the Kalman filter value of x_5 are shown in Fig. 8 (*d*).

7. Implementation at Sira-Kvina

In June 1978, the model and various utility programs were installed on a PDP 11/34 computer at the main Sira-Kvina power station in southern Norway. Much emphasis has been laid on a good man–machine communication. The implemented prediction system has the following advantages and characteristics:

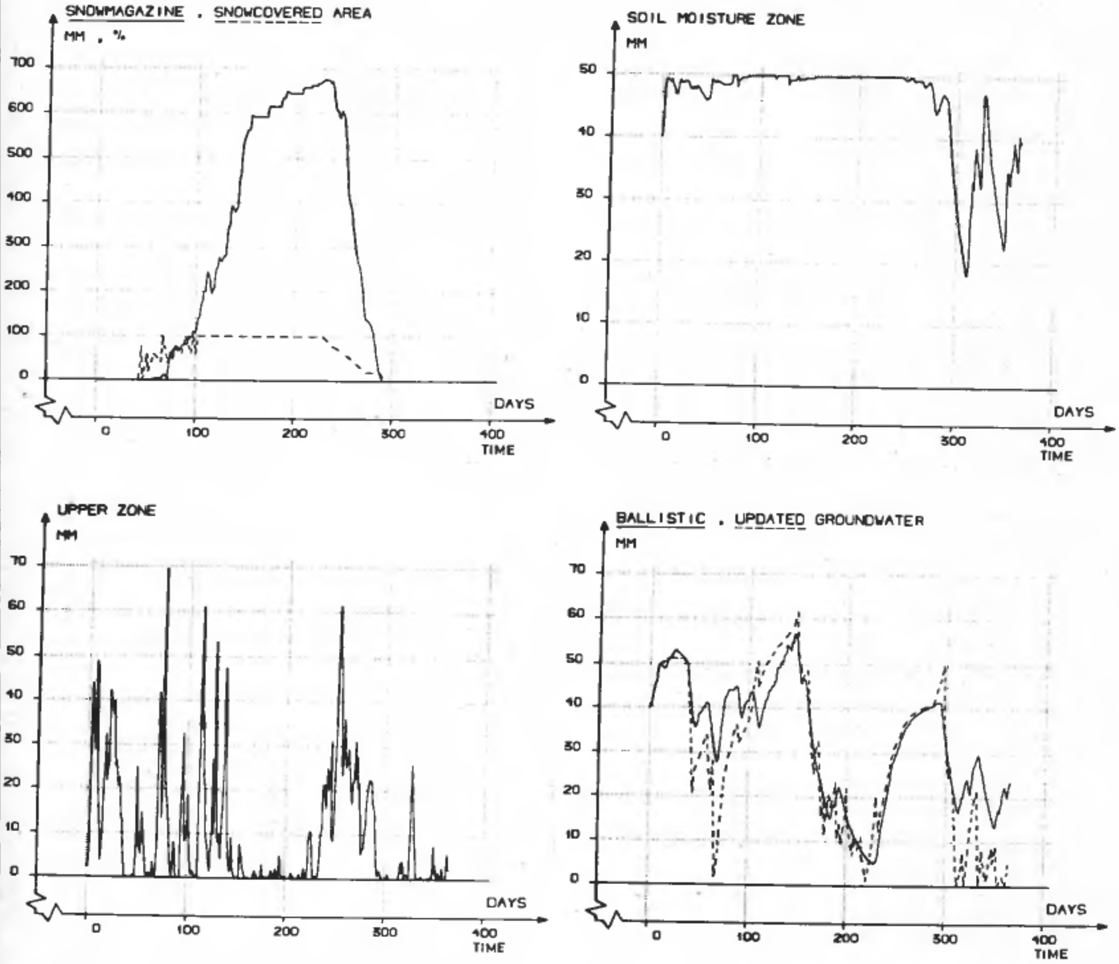

Figure 8. (*a*) Estimated $x_1 = x_2$, the total equivalent water level of the snow magazine, (*b*) estimated soil moisture zone level x_3, (*c*) estimated upper zone level x_4, (*d*) estimated groundwater zone level x_5, with ballistic model and Kalman filter.

(1) Data for observed precipitation, temperature and run-off are stored sequentially in a data base. In this data base, the *a priori* and *a posteriori* estimates of the Kalman estimated run-off are stored, too. Before the operator runs a prediction, he can observe from a graphic display how the model has performed the last few weeks, both with and without updating. The company may after a year or so request a renewed calibration of the model. All these data will be a basis for evaluating more closely the profit gained by using the model.

(2) When a prediction for the coming week is to be made, the operator will type on the keyboard the best estimates of temperature and precipitation from a weather forecast for the area. The model is then run, in steps of 1 day ahead at a time, with the initial conditions as obtained from the previous Kalman filter update (*a posteriori* estimate) obtained from the most recent measurement data.

Further, the operator may study the behaviour of the snow magazine, the soil moisture zone and the upper and groundwater zones. In this way, the model is a teaching aid in the instruction about the hydrological process.

(3) The predicted run-off updates the contents of a run-off data base, and can be directly read by another program performing a simulation of a model encompassing the complete river system of the area, the magazines and the power stations.

8. Conclusions

According to the responsible authorities at the Sira-Kvina Power Company, the prediction model has contributed to an already observable improvement in the performance of the power station and in avoiding loss of spilling water. Although some obvious shortcomings exist in the modelling today, the system is simple and highly useful in its current form.

For instance, just for one 1979 spring month the Power Company reports a very substantial increase in profit by an estimated $110 000, obtained as a difference between what they would have expected to achieve observing the historical run-off data, and what was actually achieved. This stems from an increased storage of water in the intake reservoir of Tonstad during the floods when the prices were extremely low. When the flood had ended, the saved water was sold at a much higher price.

The open-loop estimation without updating is surprisingly good compared with the Kalman filter. This is due partly to the structure of such systems in general (explained below), and partly due to the hydrology of this particular area together with a too low updating frequency.

Most hydrological models of the Nordic kind are 'excited from zero', i.e. the run-off decays close to zero for long periods of the year, being forced by impulse-like precipitation now and then. Further, a general characteristic is that strong non-linearities are experienced for high intensity rainfalls, causing fast discharge from the catchment. Thus, long-term drifts in the state variables do not exist except possibly for the groundwater zone.

The Sira-Kvina catchment is characterized by shallow soil areas and mountains. Hence, the time constants are smaller than they would be for many other interesting areas in Norway, and it should be expected that the behaviour of states in the Kalman filter will show greater differences than here compared to the ballistic estimates.

Inaccuracies introduced in the predicted run-off stem from various factors, such as a simplified model structure, a too low order of the model, errors in parameters, and too low sampling frequency in the measurements. Lack of representability in the measurement of precipitation may be a serious and systematic error source. Extrapolated temperature values for use in the multi-altitude snow model may be erroneous, and cause problems in run-off prediction during the snow season.

The latter types of errors could be classified as errors in the estimation of the total area input functions based on local point measurements of these functions.

When experience over some years is gained, *area correction factors* applied to point measurements can be estimated, since all types of precipitation somehow must finally show up in the integrated run-off.

It is important to obtain good, long-term (5 days) meteorological forecasts, since these are inputs to the model for running a predicted run-off. A cooperation with the State Meteorological Institute in Noway has been established in order to improve the forecasts for this particular area.

Regarding measurements, it is easy to suggest improvements that will improve the estimation and prediction, not considering the cost of such measurements. A more frequent updating should have high priority, a sampling interval of approximately 4 hours should be more satisfactory. During the cold seasons, it is better to measure directly the type of precipitation (rain or snow), rather than modelling it. In particular, during the spring, important information would be obtained by measuring the water originating from melted snow, and by measuring average depth of snow. Area snow coverage and its distribution could be estimated through remote sensing, and all this would make the snow magazine practically observable.

As far as modelling improvements are concerned, the mathematical description of the snow magazine has been improved. A model which takes account of different percentage area coverages of snow within each model for the various altitudes, has proved to improve prediction during the melting period.

ACKNOWLEDGMENTS

The authors are greatly indebted to the Sira-Kvina Power Company for giving permission to publish this paper, and to the financing companies and institutions. Discussions with and advice from Dr. Å. Killingtveit, Mr. B. Wingård and Mrs. M. Fossdal on hydrology are greatly appreciated.

Appendix

Approximate discrete-time state equations for a non-linear system approximated by a piecewise linear one

Consider the non-linear system

$$\dot{\boldsymbol{x}}=\boldsymbol{f}(\boldsymbol{x}, \boldsymbol{u}) \tag{A 1}$$

and an arbitrary, sufficiently short, time-interval $[k\Delta t, (k+1)\Delta T]$.

Consider a fixed value $\boldsymbol{x}_0$ of $\boldsymbol{x}$, and consider the evolution of $\boldsymbol{x}(t)$ from this point, i.e. $\boldsymbol{x}(t)=\boldsymbol{x}_0+\Delta\boldsymbol{x}(t)$. Linearizing with respect to x,

$$\Delta\dot{\boldsymbol{x}}(t)\cong A\Delta\boldsymbol{x}(t)+\boldsymbol{f}(\boldsymbol{x}_0, \boldsymbol{u}) \tag{A 2}$$

where

$$A=A(\boldsymbol{x}_0, \boldsymbol{u})=\left.\frac{\partial \boldsymbol{f}}{\partial \boldsymbol{x}}\right|_{\boldsymbol{x}=\boldsymbol{x}_0} \tag{A 3}$$

Now take $\boldsymbol{x}_0$ as $\boldsymbol{x}(k\Delta T)$, and the approximate solution for $\Delta\boldsymbol{x}$ at time $(k+1)\Delta T$ is hence

$$\Delta\boldsymbol{x}(k+1)=\exp(A\Delta T)\Delta\boldsymbol{x}(k)-A^{-1}[I-\exp(A\Delta T]\boldsymbol{f}(\boldsymbol{x}(k), \boldsymbol{u}(k)) \tag{A 4}$$

considering $\boldsymbol{f}$ as a constant vector over $[k\Delta T, (k+1)\Delta T]$, and for convenience we have used the common argument k in lieu of $k\Delta T$.

However, by definition $\Delta\boldsymbol{x}(k)\equiv 0$, and $\boldsymbol{x}(k+1)\triangleq\boldsymbol{x}(k)+\Delta\boldsymbol{x}(k+1)$, such that

$$\boldsymbol{x}(k+1)=\boldsymbol{x}(k)-A^{-1}[I-\exp(A\Delta T)]\boldsymbol{f}(\boldsymbol{x}(k), \boldsymbol{u}(k)) \tag{A 5}$$

Special case

Consider a first order system, and

$$f(x, u)=g(x)h(u)x+k(u) \tag{A 6}$$

Equation (A 5) will become

$$x(k+1)=[I-A^{-1}[I-\exp(A\Delta T)]g(x(k))h(u(k))]x(k) - A^{-1}[I-\exp(A\Delta T)]k(u(k)) \quad \text{(A 7)}$$

or

$$x(k+1)=\Phi_{x,u}(k)x(k)+\tilde{u}_{x,u}(k) \quad \text{(A 8)}$$

with the notation

$$\tilde{u}_{x,u}(k)=-A^{-1}[I-\exp(A\Delta T)]r(u(k)) \quad \text{(A 9)}$$

and

$$\Phi_{x,u}(k)=I-A^{-1}[I-\exp(A\Delta T)]g(x(k))h(u(k)) \quad \text{(A 10)}$$

The subscripts x, u are a reminder of the fact that Φ is updated in dependence of x and u.

The state equations for x_1 and x_2 in the hydrological model are of the integrator type. In that case, $\Phi(k)=I$ and $\tilde{u}(k)=\Delta T u(k)$.

Also note, if $\Delta T \to 0$, (A 5) gives the Euler method of integration.

Remark

The state equations for x_3, x_4 and x_5 in one hydrological system may be transformed to arrive at the form (A 6), by defining certain 'switching functions'.

Define

$$S(x_1)=\begin{cases}1 & \text{for} \quad x_1 \geqslant 0\\ 0 & \text{for} \quad x_1=0\end{cases} \quad \text{(A 11)}$$

$$B(x_1, x_2, \theta)=\begin{cases}1 & \text{for} \quad \theta>\theta_0 \text{ and } x_2=\alpha x_1>0;\\ & \text{or for } \theta>\theta_0 \text{ and } x_1=0\\ 0 & \text{otherwise}\end{cases} \quad \text{(A 12)}$$

In its time-discrete form, and applying (A 5), eqn. (3) in the paper may then be expressed for $x_3<x_{3\max}$ as

$$x_3(k+1)=x_3(k)+\frac{1-\exp[-a(k)\Delta T]}{a(k)}\Big\{[1-x_{3\max}{}^{-\beta}\, x_3(k)^{\beta}] \times B(x_1(k), x_2(k), \theta(k))[S(x_1(1))C_0[\theta(k)-\theta_0](1+\alpha_w)+P(k)] - (1+\alpha)x_3(k)/x_{3\max}q_{2\mathrm{pot}}(k)\Big\} \quad \text{(A 13)}$$

where

$$a(k)=x_{3\max}{}^{-\beta}\, \beta x_3(k)^{\beta-1}B(x_1(k), x_2(k), \theta(k)) \times [S(x_1(k))C_0[\theta(k)-\theta_0](1-\alpha_w)+P(k)]+(1+\alpha)\frac{q_{2\mathrm{pot}}}{x_{3\max}} \quad \text{(A 14)}$$

For $x_3 \geqslant x_{3\max}$,

$$x_3(k+1)=x_3(k)-q_{2\mathrm{pot}}\Delta T \quad \text{(A 15)}$$

Equation (6) may be expressed as

$$\dot{x}_4 = -b(x_4) + c \tag{A 16}$$

or in time-discrete form

$$x_4(k+1) = \exp\,[-b(k)\Delta T]x_4(k) + \frac{1-\exp\,[-b(k)\Delta T]}{b(k)}c(k) \tag{A 17}$$

$c(k)$ is a function of $x_3(k)$, $\theta(k)$ and $P(k)$. $b(k)$ is independent of θ and P.

For (A 17) the following four situations are possible.

(1) $x_4 \geqslant x_{4\max}$, $x_3 < x_{3\max}$: then $b = a_1 + a_2$, and

$$c(k) = a_1 x_{4\max} - \frac{q_4}{1-\alpha_L} + x_{3\max}{}^{-\beta}\, x_3(k)^{\beta} B(x_1(k), x_2(k), \theta(k)) \times [S(x_1(k))C_0[\theta(k) - \theta_0](1+\alpha_w) + P(k)] \tag{A 18}$$

(2) $x_4 < x_{4\max}$, $x_3 < x_{3\max}$: then $b = a_2$, and

$$c(k) = -\frac{q_4}{1-\alpha_L} + x_{3\max}{}^{-\beta}\, x_3(k)^{\beta} B(x_1(k), x_2(k), \theta(k)) \times [S(x_1(k))C_0[\theta(k) - \theta_0](1+\alpha_w) + P(k)] \tag{A 19}$$

(3) $x_4 > x_{4\max}$, $x_3 \geqslant x_{3\max}$: then $b = a_1 + a_2$, and

$$c(k) = -\frac{q_4}{1-\alpha_L} + a_1 x_{4\max} + B(x_1(k), x_2(k), \theta(k)) \times [S(x_1(k))C_0[\theta(k) - \theta_0](1+\alpha_w) + P(k)] \tag{A 20}$$

(4) $x_4 < x_{4\max}$, $x_3 \geqslant x_{3\max}$: then $b = a_2$, and

$$c(k) = -\frac{q_4}{1-\alpha_L} + B(x_1(k), x_2(k), \theta(k)) \times [S(x_1(k))C_0[\theta(k) - \theta_0](1+\alpha_w) + P(k)] \tag{A 21}$$

The time-discrete solution of (6) is

$$x_5(k+1) = \exp\,(-a_3\Delta T)x_5(k) + \frac{1-\exp\,(-a_3\Delta T)}{a_3}[q_4 + \alpha_L(P(k) - q_{2\mathrm{pot}}(k))] \tag{A 22}$$

The equations for x_3 and x_4 can now be cast in the form of (A 6).

$\Phi_{x,u}$ turns out to be of the form

$$\Phi_{x,u} = \begin{bmatrix} 1 & 0 & 0 & 0 & 0 \\ 0 & 1 & 0 & 0 & 0 \\ 0 & 0 & \varphi_{33}(k) & 0 & 0 \\ 0 & 0 & \varphi_{43}(k) & \exp\,(-b(k)\Delta T) & 0 \\ 0 & 0 & 0 & 0 & \exp\,(-a_3\Delta T) \end{bmatrix} \tag{A 23}$$

where φ_{33}, φ_{43} and b are certain functions of the operating point and system parameters.

The remaining part of each state eqn. (16) constitutes the forcing term $\tilde{u}_i$. These terms, however, will not be given here.

With the obtained expressions for $\Phi_{x,u}$ and $u_{x,u}$ in (16), the set of equations was solved with field data for precipitation, temperature and evapo-transpiration based on hydrological estimates.

The resulting functions $x(k)$ were compared with a fourth-order Runge–Kutta method with a fixed step length, applied to the set (1), (2), (4), (6) and (7). The discrete-time version (A 8) turned out to compare favourably in solution performance even with ΔT as long as 1 day.

However, we use the discrete-time version of the set of equations only as a basis for the computation of the estimator gain matrix.

References

AAM, S., WINGÅRD, B., KILLINGTVEIT, Å., FOSSDAL, M., and FJELD, M. (1977). A hydrological model for use in the running of hydroelectric power stations (in Norwegian). Report from EFI/NVE/IFV/SINTEF, January.

BERGSTRÖM, S. (1975). The development of a snow routine for the HBV-2 model. *Nordic Hydrology*, **6**, no. 2.

BERGSTRÖM, S., and FORSMAN, A. (1973). Development of a conceptual deterministic rainfall run-off model. *Nordic Hydrology*, **4**, no. 3.

CRAWFORD, N. H., and LINSLEY, R. K. (undated report). Digital simulation in hydrology: Watershed model IV. Technical Report 39, Department of Civil Engineering, Stanford University, California, U.S.A.

EYKHOFF, P. (1974). *System Identification, Parameter and State Estimation* (New York: Wiley).

FJELD, M., MEYER, S. L., and AAM, S. (1973). Mathematical modelling of a nordic hydrological system, and the use of a simplified run-off model in the stochastic optimal control of a hydroelectrical power system. Paper presented at the 5th IFIP Conference on Optimization Techniques, Rome, 7–11 May.

FJELD M., and SANDE, T. (1972). Value analysis and control of the power production (in Norwegian). *Elektroteknisk Tidsskrift*, **7**, 27–29.

HALLINGSTAD, O. (1976). Maximum likelihood identification of parameters in nonlinear state space models. Report STF48 A76061, SINTEF, Trondheim, Norway.

KASHYAP, R. L., and RAO, A. R. (1972). Real time recursive prediction of river flows for optimal operation of water resource systems. Paper 9.4 at the 5th IFAC World Congress, Paris, 12–17 June.

MEYER, S. L. (1972). Design of mathematical models for run-off prediction (in Norwegian). M.Sc. Thesis, Division of Engineering Cybernetics, The Norwegian Institute of Technology, Trondheim, Norway.

SCHWEPPE, F. (1973). *Uncertain Dynamic Systems* (Englewood Cliffs: Prentice-Hall).

TSE, E. (1974). Information matrix and local identifiability of parameters. JACC preprints, pp. 611–619.

TYSSØ, A. (1977). CYPROS. Cybernetic program library. Report 77-84-W, August, The Norwegian Institute of Technology, Division of Engineering Cybernetics, Trondheim, Norway.

VANSTEENKISTE, G. E. (editor) (1976). *System Simulation in Water Resources* (Amsterdam: North-Holland).